JOURNAL OF THERMOPHYSICS AND HEAT TRANSFER
Vol. 17, No. 2, April–June 2003

Temperature Distribution in a Composite Box Structure Subject to Transient Heat Fluxes

J. R. Miller* and P. M. Weaver†
University of Bristol, Bristol, England BS8 1TR, United Kingdom

Finite element and analytical approaches are used to determine the transient temperature distribution through an air-filled box structure with carbon-fiber-reinforced plastic skins. A study of the individual and combined effects of conduction, convection, and radiation boundary conditions is performed. A novel method for the inclusion of natural convection within a cavity using the finite element program ABAQUS is presented. It is shown that although the effects of natural convection within the cavity are less significant than that of radiation, they are not negligible and, thus, should not generally be excluded from the analyses. Analytical models based on integral transforms are developed to describe the temperature distribution through the skin, subject to combined thermal loading conditions. Fully transient convection conditions as well as combined semitransient convection–radiation conditions are modeled, and the limits of this analytical solution are explored. The analytical modeling of combined convection and radiation conditions using integral transforms is novel and is shown to predict temperatures within approximately 5°C of those given by finite element analyses.

Nomenclature

H	=	h/k, m^{-1}
h	=	heat transfer coefficient, W/m^2K
h_c	=	convection heat transfer coefficient, W/m^2K
h_R	=	equivalent radiation heat transfer coefficient, W/m^2K
k	=	conductivity, W/mK
L	=	skin thickness, mm
m	=	number of series terms
q	=	heat flux, W/m^2K
T	=	temperature, K
T_i	=	initial temperature at $t = 0$, K
T_s	=	surface temperature, K
T_∞	=	sink or reference temperature, K
t	=	time, s
x	=	position through thickness of skin, mm
α	=	thermal diffusivity, m^2/s
β_m	=	eigenvalues
ε	=	surface emissivity
σ	=	Stephan–Boltzmann constant, $5.669e^{-8}$ W/m^2K^4

Introduction

THE use of composites, especially carbon-fiber reinforced plastics (CFRP), in challenging temperature environments such as aircraft and space operations, continues to increase. Understanding the structural behaviour of these materials within extreme environments is of paramount importance. Before this behavior can be examined, however, it is necessary to be able to predict accurately the temperature through a structure. The objective of the current work was to study a large box structure made of composite skins and filled with air, subject to conduction, convection, and radiation boundary conditions. Such a structure is representative of a composite aircraft wing. The aim was to gain an understanding of the effects of each individual heat transfer mechanism and predict surface and through thickness temperature profiles for the box structure using analytical and finite element (FE) models for comparison.

In reality, the thermal boundary conditions are generally a combination of conduction, convection, and radiation. To gain meaningful results, it is expected that all of these conditions should be modeled in a transient fashion. Figure 1 shows the boundary conditions involved in the problem of a box structure.

Transient temperature analyses for box structures, especially those constructed of composite materials and under a wide range of thermal conditions, are largely unavailable in the open literature. Steady-state analysis has been performed,[1] but transient models including all modes of heat transfer are few. Natural convection models within a cavity, or box structure, with a temperature difference between horizontal walls are also scarce. Generally, the natural convection models that exist are either for small enclosures[2] or involve an incomplete cavity[3] subject to boundary conditions quite different from those of the current problem. The inclusion of radiation effects in a cavity has been studied, but the results of such studies are generally too specific to be applied to a problem involving combined mechanisms of heat transfer.[4] No work was found in the open literature that combined the effects of transient natural convection and radiation within a horizontal box structure, and none of the mechanisms of heat transfer studied independently involved work on composite structures.

In most current analyses, numerical solutions, such as FE analyses, are adopted as the method of predicting temperature profiles. This is accepted as an accurate method in general heat transfer analyses. However, analytical analysis may also be considered as a viable method of solution, which often offers greater physical insight to the problem than numerical analysis. Although analytical methods are commonplace, the use of these methods is generally limited to simplified, less realistic boundary conditions for steady-state analyses. The integral transform solution technique, which is well described by Osizik,[5] is known to be an effective method of analytical analysis that can, in theory, be adapted to suit most boundary condition combinations. Generally, however, the potential for using this method is not fully explored. Some analytical solutions have been formed for transient problems using this technique, but these are most often limited to semi-infinite or infinite solids where exact,[6] rather than series, approximations can be obtained. For the limited work that has been done on plates with finite boundaries, simplified boundary conditions of constant temperature or constant flux are applied.[7–9] There are a few papers containing models with convection conditions[10,11]; however, the inclusion of radiation boundary conditions along with convection has not been explored.

Received 18 April 2001; revision received 17 June 2002; accepted for publication 22 October 2002.

*Graduate Student, Department of Aerospace Engineering, Queens Building, University Walk; Jodi.Zelenski@bristol.ac.uk.

†Lecturer, Department of Aerospace Engineering, Queens Building, University Walk; Paul.Weaver@bristol.ac.uk.

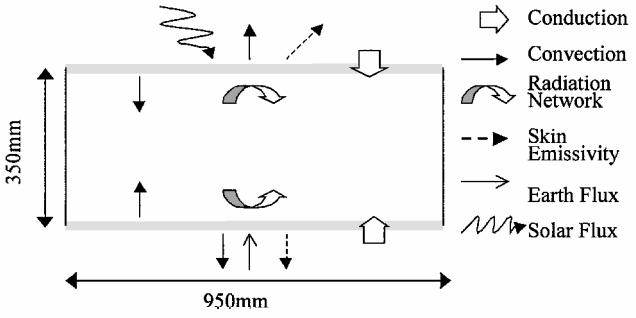

Fig. 1 Thermal loading conditions.

This paper presents a method of transient temperature prediction through a simplified CFRP air-filled box structure, by use of FE and analytical analysis. FE analysis is used to model the global structure subject to the complete range of conduction, convection, and radiation boundary conditions. An analytical model based on integral transforms is then developed to compare with FE results for the temperature profile through the bounding skin itself. The analytical model expands on previous work[5,10,11] to include radiation boundary conditions.

Global FE Model

Model Description

A FE model based on the box structure with dimensions described by Fig. 1 was developed. The model was made up of DC2D8, two-dimensional ABAQUS heat transfer elements. In this model the skins were assumed to be CFRP and were modeled with four elements through the thickness. The space contained between the CFRP was modeled with eight elements through the thickness. These elements were given the material properties of air, and the size of the elements was graduated such that smaller elements were located directly below the skin surface and the elements got progressively larger toward the midplane. There were 50 elements, each of equal width, used across the width of the box to ensure that no edge effects were present at the centerplane, where the temperatures were considered. The internal surfaces were assumed to be smooth for the purpose of radiation, and there were assumed to be no internal obstructions such that every surface within the box could reflect radiation to every other surface. Previous runs with coarser meshes showed that mesh effects had been eliminated.

The CFRP was assumed to be homogeneously orthotropic, and the material properties were those of a layup consisting of 50% 0-deg fibers, 40% 90-deg fibers, and 10% ±45-deg fibers in an epoxy resin. The material properties in the lengthwise (direction 1) and through thickness (direction 2) directions, respectively, were assumed to be uniform. The material properties for CFRP[12] and air[13] used in the various analyses can be seen in Table 1. Properties are given at two temperatures, 270 and 500 K. The properties at temperatures between these values were calculated by linear interpolation. A very hot, dry 12-h day was chosen for the model temperature conditions. The effects of conduction, convection, and radiation on external skin surfaces and within the tank were studied.

To model the external thermal loads as shown in Fig. 1, the standard equations of heat transfer given by Holman[6] for conduction (1), external convection (2), and external radiation (3) conditions were applied by ABAQUS[14] within the model as

$$q = -k\frac{\mathrm{d}T}{\mathrm{d}x} \tag{1}$$

$$q = h(T_s - T_\infty) \tag{2}$$

$$q = \sigma\varepsilon\left(T_s^4 - T_\infty^4\right) \tag{3}$$

Solar radiation was considered as the primary method of external heating, and it was assumed that there was no internal heat generation within the box structure. A sine wave with a maximum value of 1000 W/m^2 and a period of 12 h, beginning at 0600 hr, was used to represent the solar flux on the top surface. A resultant solar flux was calculated for the bottom surface using an Earth emissivity of 0.67. Temperatures obtained from previous experimental measurements in a hot dry environment[13] were used as the sink temperatures, as shown in Fig. 2. The "air" temperature was used for external convection, the "internal" temperatures were calculated based on results from conduction-only analysis, the "sky" temperature is a measured atmospheric level temperature used for radiation to the top skin, and "Earth" is measured on a grey concrete surface and used for radiation to the bottom skin. Natural convection was the only form of convection present on the skin surfaces, that is, windless, worst-case conditions. The lateral bounding surfaces of the model were considered insulated at their external faces, which is similar to having unidirectional CFRP at these vertical faces due to its extremely low conductivity (typically $k < 1$ W/m^{2}K).

Table 1 Material properties

Property	CFRP	Air[a]
Emissivity	0.8	——
Conductivity (270 K), W/mK		
Direction 1	8.38	0.0237
Direction 2	0.81	0.0237
Conductivity (500 K), W/mK		
Direction 1	11.99	0.037
Direction 2	1.37	0.037
Specific heat, J/kg K		
270 K	848	1011
500 K	1485	1011
Density, kg/m^3		
270 K	1550	1.252
500 K	1550	0.723

[a]All values for air properties are given at 273 and 473 K rather than 270 and 500 K, respectively.

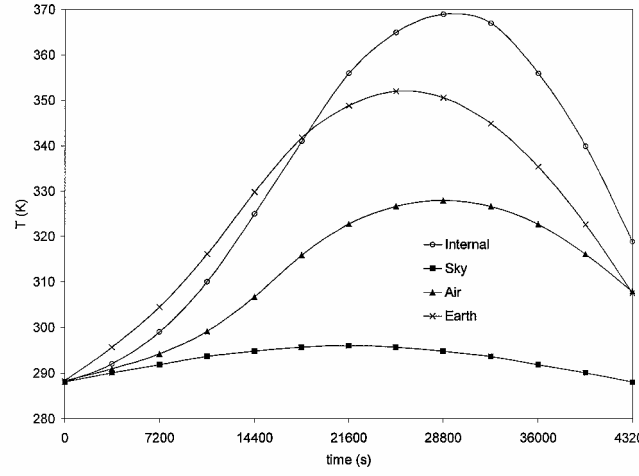

Fig. 2 Sink temperatures for convection (air) and radiation (sky) over a 12-h period.

Conduction-Only, Convection-Only, Radiation-Only, and Combined Convection–Radiation Analyses

Within the tank, individual studies were made for each of the three mechanisms of heat transfer: conduction, convection, and radiation. Equation (1) was applied quite simply to model conduction through the tank. Radiation within a cavity requires additional equations, but ABAQUS has the capability to perform this type of analysis. Based on viewfactor calculations and material emissivities, ABAQUS assesses the potential of each surface to absorb, transmit, and reflect radiation to every other internal surface, which can then in turn, absorb, transmit, and rereflect this radiation. ABAQUS's capability to model convection within an enclosure or cavity, however, is limited to forced convection; thus, an alternative approach, similar to the that used for external convection conditions, was adopted to account for natural convection within the box structure.

The convection heat transfer coefficient for each surface was calculated using a number of different approaches. Fujii and Imura[15] have determined three equations for upward and downward facing plates. These equations have been generally accepted for use with air as the convection fluid based on the correlation of independent experiments, as summarized by Holman.[6] Equations determined by Singh et al.[16] and Vilet[17] were also used as comparison. Based on convection heat transfer work studying edge effects,[18] the significant distance between vertical boundaries, and the large number of elements horizontally, the top and bottom skins were treated as upward- or downward-facing infinite plates, depending on the thermal environment. Internally, the significant distance (approximately 0.5 m) between the top and bottom tank walls permitted the skins to be treated as two infinite plates with separate thermal environments. This assumption was justified through a comparison of conditions in previous studies of convection within air- and water-filled enclosures.[19,20] The internal surface temperatures were determined by performing a heat transfer analysis of the wingbox model, where the only method of heat transfer within the tank was conduction. This was considered to be the highest possible temperature scenario because the air acts as an insulator inside the tank due to its low conductivity. This implies that the hottest temperatures occur at the internal surface of the bounding skins. To make use of this worst-case scenario, these temperatures at the internal skin surfaces were used as the sink temperatures for the separate thermal environments. This assumption is valid because in a conduction-only analysis the gradient remains linear and this opposing surface is the boundary of this gradient, thus dictating the "far-field" temperature.

The error associated with using a formula to find the heat transfer coefficient can be substantial, due to the specific experimental conditions used in each particular case and with the addition of experimental error itself. These potential sources of error are generally well realized, and errors of up to approximately 20%, depending on the severity of the approximations made for the given problem, have been suggested as a safe estimate when using the convection heat transfer coefficient equations.[6] When this 20% error approximation was used, the bounds of the prospective heat transfer coefficients were calculated, and the most conservative values were used to provide a worst-case or highest temperature scenario.

In the present analyses, heat transfer coefficients of 8 and 3 W/m^2K were calculated, using the aforementioned methods, for the top and bottom external surfaces, respectively, with the surrounding air temperature as the sink temperature over the 12-h period, as shown in Fig. 2. In the case of radiation at the external surfaces, the sink temperatures used were the sky temperature, because it is closer to the sun for the top surface, and the Earth temperature because it is the nearest source of radiation for the bottom surface. It was assumed that there were no clouds to interfere with the sun's radiation, no radiation was incident from other sources, and radiation was not rereflected from the Earth back to the bottom surface.

Internally, a value of 2 W/m^2K was found, based on sink temperatures from the conduction-only analysis. This value was used for the first 9 h on the top surface, during which this surface was at a hotter temperature than the bottom surface according to preliminary conduction-only analysis. Throughout this period, no natural convection was assumed to take place at the bottom surface because the thermal gradient can only act in one direction. As stated, the temperature of the bottom surface obtained via a conduction-only analysis for the corresponding time was used as the sink temperature. These values correspond to the first eight points of the internal curve of Fig. 2. For the last 3 h of the analysis, when the bottom internal surface was found to be hotter, a value of 4 W/m^2K was applied to the bottom internal surface, with zero convection heat transfer on the top surface. The sink temperatures were the internal top surface temperatures, which correspond to the last four points of the internal curve of Fig. 2. Radiation was calculated internally by ABAQUS after defining the internal surfaces and their material properties.

The heat transfer coefficients are a function of surface temperatures, which are known to vary throughout the day, suggesting that the heat transfer coefficients will also vary. This effect was examined, and 12 different heat transfer coefficients were used over the course of the 12-h day to represent this effect. The results of this analysis, however, showed negligible changes from those analyses that used a constant heat transfer coefficient throughout the day. Based on the error associated with the calculation of the heat transfer coefficients and the minimal influence in the results, it was determined that no noticeable improvement in accuracy was gained by varying the heat transfer coefficients, and thus, they were held constant for all analyses.

FE Results

The simplest form of analysis completed involved conduction as the only method of heat transfer through the box. Not surprisingly, this resulted in the highest temperatures. The poor conductivity of the air acted as an insulator on the internal skin surfaces, not permitting any heat to be removed from the skins. The next type of analysis included the effects of natural convection within the cavity. This inclusion had a small effect on the temperature observed; however, the effects were not considered negligible.

Finally, an analysis including only radiation within the tank was performed. These results showed the largest temperature changes in comparison to the conduction-only analysis and can be explained by the fourth-order radiation effects. Because of the large difference between the surface and sink temperatures, the fourth-order power of these temperatures make this difference even more significant, which in turn lead to increased cooling of the skins due to radiation. Once these analyses with only one internal boundary condition had been completed, an analysis using combined internal convection and radiation was performed. This combined analysis resulted in a further reduction in the overall maximum temperatures, which occur at the top surface. Figure 3 shows the results of these analyses.

The analysis reaches a time, at approximately 1400 hr, when the bottom skin becomes hotter than the top skin. Although the maximum solar flux occurs at 2400 hrs, the Earth flux lags the solar flux by approximately 2 h due to the absorption and emittance of incoming radiation. Because the temperature of the bottom surface is primarily dictated by the behavior of the Earth, the reversal in the position of the maximum temperature follows the same pattern. Up to this reversal time, the conduction-only analysis produces the highest temperatures for the top skin, but the radiation-only analysis, in comparison, produces the higher temperatures on the bottom skin. This is because, for the radiation analysis within the cavity, the emittance of radiation is only a function of temperature gradient. Therefore, because the top skin is at the higher temperature, it can effectively emit radiation as a way of cooling the surface, leading to lower temperatures than with the conduction-only analysis. The bottom skin, on the other hand, is forced to absorb this incoming radiation because of its lower temperature, and the only way it can slightly cool itself is to reflect some of the radiation back toward the top skin. Because it cannot actually emit radiation at this time, the bottom skin heats up and, in doing so, explains the higher temperatures of the radiation-only analysis. After this reversal time, the effects of conduction-only and radiation-only are seen to reverse for

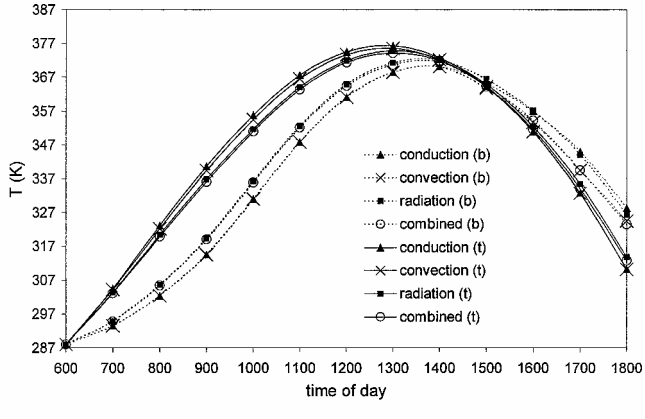

Fig. 3 Results of individual heat transfer mechanism analyses, where (t) is top surface and (b) is bottom surface.

the top and bottom skins. Again this can be explained by the hotter bottom surface having the ability to emit radiation.

From Fig. 3, it can also be seen that the convection-only and conduction-only trends for both the top and bottom surfaces are very close together at all times, suggesting that the cooling effects of the internal convection are small, but as can be deduced from the combined plots, not insignificant because the combined results do not follow exactly the radiation-only trend.

Before the reversal time, radiation is seen to have a significant cooling effect on the top skin, but the convection actually causes an increase in the temperature due to the very small heat transfer coefficient acting more like an insulator. After the reversal time, however, convection cooling occurs, and heating this time is due to radiation. On the bottom skin, convection has a negligible effect, in comparison to radiation, up to the reversal time; however, after this time the analysis is dominated by convection. This increase in effect of the convection on the bottom skin as compared with the top skin is explained by that the transfer coefficient is more than double that of the top skin.

Examples of the FE results for the combined temperature profiles are given in Fig. 4. The curvature seen at the horizontal edges is caused by no boundary conditions being specified at these edges; therefore, ABAQUS sees them as perfectly insulated. Some of these edge effects may also be due to rereflection of radiation. This condition is similar to having unidirectional CFRP boundaries. Temperature results for these analyses were based on the uniform distribution through the center of the structure.

Global Model Conclusions

To obtain a realistic and accurate temperature prediction model, the internal boundary conditions of natural convection and cavity radiation should be included. In an air-filled box, the top surface temperature is greater than the bottom surface temperature up to the reversal time, approximately 1400 hr, after which the bottom surface becomes hotter. The position of the maximum temperature associated with the "reversal time" corresponds directly with the external flux behavior.

The highest maximum skin temperatures were approximately 105 and 98°C (378 and 371 K) on the top and bottom skins, respectively. These high temperatures were due to the insulating characteristics of the air within the box structure, preventing the efficient dissipation of heat. Radiation was seen to have a large influence in these temperature profiles, especially before the reversal time. Convection was also found to play a role, particularly after the reversal time, vindicating its inclusion in the model.

Analytical Model Through Skin

Integral Transforms

To keep a global model efficient, few elements can be used through the skin, thus limiting the understanding of the behavior in this critical area. A local model is, therefore, required. A FE model of this area is trivial, but requires redesign each time a dimensional parameter is changed. An analytical model can generally eliminate the requirement for redesign and, from an academic point of view,

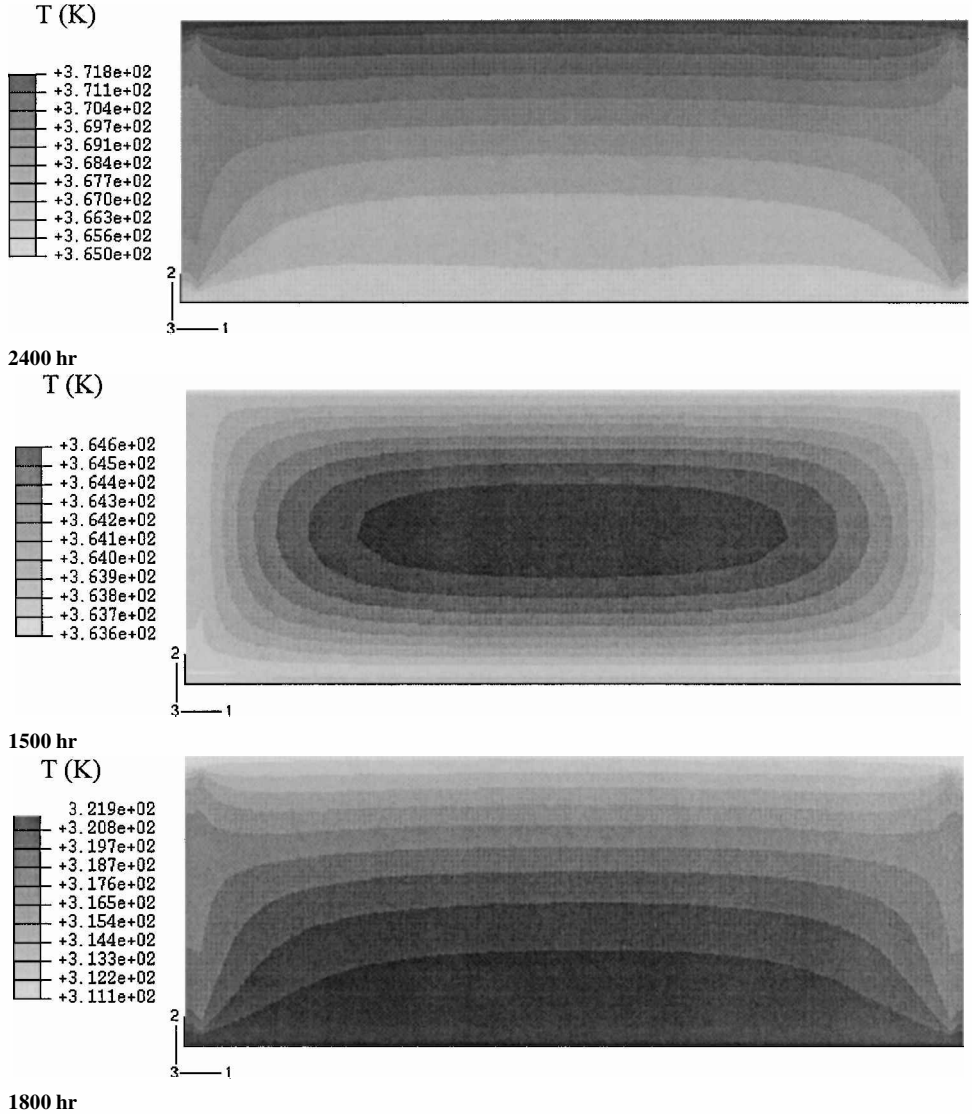

Fig. 4 FE temperature profiles.

offers greater insight to the problem. The analytical model developed herein is modeled using integral transforms as discussed by Osizik.[5] Convection conditions were examined first, and compared with FE and Heisler chart (see Ref. 6) results. These conditions were then further developed to offer improved usability over the Heisler chart method. Based on work by Zerkle and Sunderland,[21] a novel linearized form of radiation boundary conditions was developed for modified use with the analytical model for convection. Finally, the effects of combined convection–radiation conditions were considered.

The local model of the top skin can be seen in Fig. 4, whereas the basic Fourier heat transfer equations used to describe the current problem with convection-only boundary conditions are given by

$$-k_1(t)\frac{\mathrm{d}T}{\mathrm{d}x} + h_1(t)T = h_1(t)T_{\infty 1}(t) \qquad \text{at} \qquad x = 0 \tag{4}$$

$$k_2(t)\frac{\mathrm{d}T}{\mathrm{d}x} + h_2(t)T = h_2(t)T_{\infty 2}(t) \qquad \text{at} \qquad x = L \tag{5}$$

$$T = T_i \qquad \text{at} \qquad 0 \le x \le L, \quad t = 0 \tag{6}$$

The variable $k_n(t)$ is the conductivity of the solid of surface n as a function of time and similarly for all other variables.

The development of temperature profile equations rely on integral transforms and inversion formulas as given by Osizik.[5] Integral transforms are limited to linear boundary conditions.[5] Osizik's formulas have been used as a benchmark for other analytical developments.[10,11] These further developments have only taken place in recent years, which suggests that the potential use of analytical solutions, rather than numerical analysis, has not been fully explored. The difficulty in approaching heat transfer problems with an analytical method is that, for any small alteration in the problem definition, especially the boundary conditions, the analytical solution may change dramatically.

The concepts and nondimensionalised formulation of a general analytical solution are quite straightforward, as de Monte[10] suggests. De Monte gives a good summary of the different possible analytical methods that could be used to solve transient heat transfer problems, as well as their strengths for specific applications. The error analysis performed is valuable in gaining an appreciation for the number of terms required to reach a desired level of accuracy using the closed-form analytical solution. Unfortunately, in the problem definition itself, a simplifying assumption of constant temperature boundary condition is made, limiting the applicability of the work for more complicated problems. Antonopoulos and Tzivanidis[11] have also carried out analysis using the integral transform technique. Analytical solutions were developed for one-dimensional heat transfer through a composite structure, subject to convection boundary conditions at its surfaces. The model provides important insight to analytical solutions in a composite region, but it does not address radiation boundary conditions, which are known to have a significant effect in the current problem.

Convection Boundary Conditions

In the first development of an analytical solution for third-order, convection boundary conditions at both external surfaces as seen in Fig. 5, certain simplifying assumptions were made. The skin was considered as a homogeneous material; thus, k_1 and k_2 were equal. The convection heat transfer coefficients on both external surfaces, the sink temperatures, and the conductivity were not varied with time. The sink temperatures used at the external surfaces was chosen as a constant $T_\infty = 323$ K for both the top and bottom surfaces.

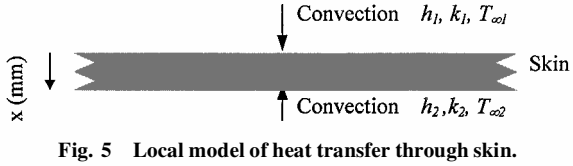

Fig. 5 Local model of heat transfer through skin.

Under boundary conditions of convection to the environment on both top and bottom of the skin, and with the assumptions as already stated, the analytical equation developed using Osizik's[5] method to describe the temperature profile through the skin is as follows:

$$T(x,t) = \sum_{m=1}^{\infty} \frac{2[\beta_m \cos(\beta_m x) + H_1 \sin(\beta_m x)]}{\left\{\left(\beta_m^2 + H_1^2\right)\left[L + H_2/\left(\beta_m^2 + H_2^2\right)\right] + H_1\right\}} \times \left(T_i e^{-\alpha\beta_m^2 t} \times \left[\sin(\beta_m L) - \frac{H_1}{\beta_m}\cos(\beta_m L) + \frac{H_1}{\beta_m} \right] + \left(1 - e^{-\alpha\beta_m^2 t}\right)\left\{ \frac{H_1 T_{\infty 1}}{\beta_m} + \frac{H_2 T_{\infty 2}}{\beta_m^2}[\beta_m \cos(\beta_m x) + H_1 \sin(\beta_m x)] \right\} \right) \tag{7}$$

The solution of the eigenvalues β_m are the positive roots of the following transcendental equation:

$$\tan(\beta_m L) = \frac{\beta_m (H_1 + H_2)}{\beta_m^2 - H_1 H_2} \tag{8}$$

Conditions of $h_1 = h_2$ and $T_{\infty 1} = T_{\infty 2}$ were chosen so that results can be compared with FE and Heisler chart (see Ref. 6) results. Simple Heisler charts can only be used to estimate the midplane temperature at a given time in the analysis. These charts often provide a larger degree of uncertainty because the user must interpolate from the charts. Furthermore, the use of Heisler charts is restricted to a specific class of boundary conditions. The analytical model developed by the use of integral transforms has a much broader range of application. Whereas the applicability of Heisler charts is limited to identical boundary conditions on both sides of the finite plate, the current analytical model has the capability to include different boundary conditions at each edge as well as time-dependent heat transfer coefficients and transient sink temperatures. FE models are also a popular method of conducting heat transfer analysis. A comparison of the three methods for convection boundary conditions, as described by Eq. (7), can be seen in Fig. 6.

There are two main sources of error associated with the analytical model: the series truncation and the calculation of the β_m eigenvalues. An infinite series would, in theory, provide exact temperature values, whereas a shorter truncated series would provide an approximation of the temperature in a reasonable computing time. Obviously, the tradeoff is accuracy to run time.

Table 2 shows a comparison of the results calculated using m terms in the series with those found by FE analysis at a given time. It can be seen in Table 2 that terms above $m = 1000$ do not contribute to improving the accuracy of the analytical results. The values given for $m = 100$ appear to be the closest match to the FE values, suggesting

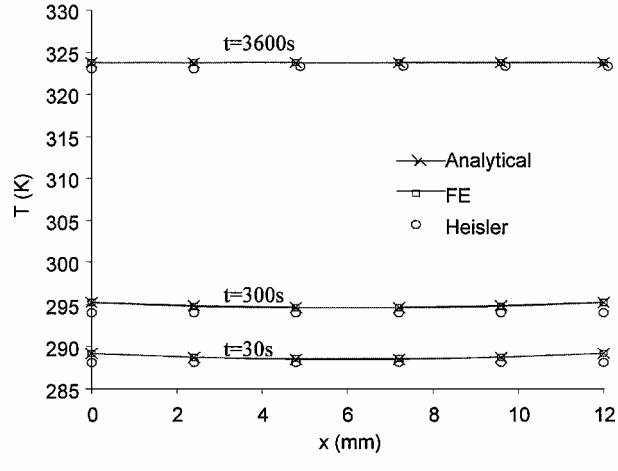

Fig. 6 Through thickness skin temperatures for identical convection boundary conditions.

Table 2 Error associated with truncation of the series after *m* terms

	T, K						
t, s	FE	$m=5$	$m=50$	$m=100$	$m=500$	$m=1{,}000$	$m=10{,}000$
30	289.2	288.25	289.12	289.17	289.21	289.22	289.22
300	295.2	294.28	295.25	295.20	295.24	295.25	295.25
3600	323.8	322.88	323.75	323.80	323.84	323.84	323.84

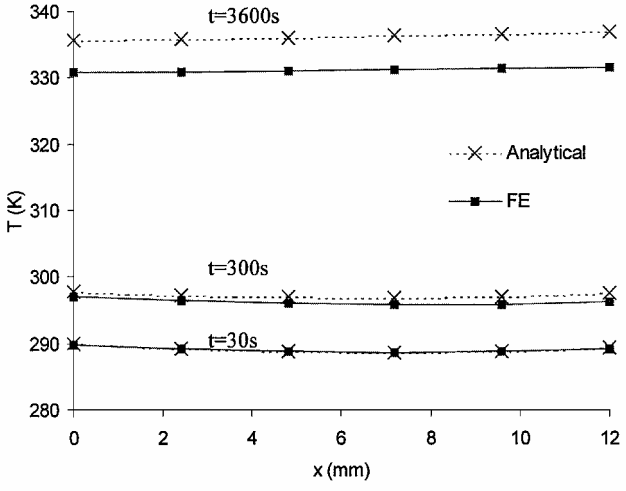

Fig. 7 Through thickness skin temperatures for different convection boundary conditions.

that the FE analysis also contains truncation errors. Thus, given these results, in future analytical models, $m = 1000$ is used. The run times associated with this number of series terms remains within an acceptable range, although it can be approximately 50% higher than that of the FE analyses.

The second source of error is the calculation of the β_m values. This was found to have an impact on overall accuracy. Because of the ill conditioning of the transcendental equation, the β_m values were required to be obtained using double precision accuracy. This, however, did not eliminate all errors in obtaining the final $T(x, t)$. Because of the inherent sensitivity of the equation, the approximation of a series for the calculation of the terms containing cosine or sine, perfect convergence of the solutions could not be reached, regardless of the number of terms used in the series. These errors, although present, are not estimated to be large, nor are they expected to be greater than those numerical errors associated with the FE analysis.

After confidence was gained in the analytical model's capabilities, the heat transfer coefficients and sink temperatures were altered at each surface to replicate conditions of different boundary conditions at the internal and external surfaces of the skin for a box structure. However, their values were still held independent of time. For this study the sink temperature for the top surface was $T_\infty = 328$ K, the maximum value of the air curve from Fig. 2 and for the bottom surface, $T_\infty = 369$ K, the maximum value of the internal curve from the global conduction-only analysis as seen in Fig. 2. Figure 7 shows a comparison of these new conditions with FE results.

The differences between the analytical results and the FE results are more profound than in the preceding case. The discrepancy appears to grow as the time increases, to a maximum difference of approximately 5 deg at steady state. This expanding difference in values results because, as time increases, the influence of the second term in the analytical series (7) increases; $(1 - e^{-\alpha\beta_m^2 t})$ $(H_1 T_{\infty 1}/\beta_m + \cdots)$. Because this second term accounts for the effects of different sink temperatures and convection heat transfer coefficients, the difference in values resulting from the errors associated with the analytical model become more significant with time. However, the steady-state value can be taken as worst case. Even at this maximum value, the discrepancy is still within 5%, and given the uncertainty associated with the heat transfer coefficients used, this falls within an acceptable range.

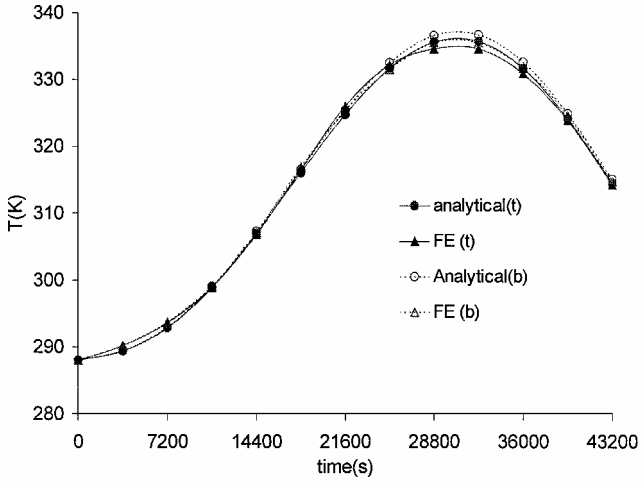

Fig. 8 Top (t) and bottom (b) skin surface temperatures for transient sink temperatures.

Next, the sink temperatures were considered functions of time as in the global analysis and represented by a fifth-order polynomial. The convection heat transfer coefficients were held constant with respect to time because, as was proven in the global box analyses, the variation of these parameters with time had negligible effect on the temperature profiles. The following equation shows the adapted version of Eq. (7) to accommodate varying sink temperatures over the course of the day:

$$T(x,t) = \sum_{m=1}^{\infty} \frac{2[\beta_m \cos(\beta_m x) + H_1 \sin(\beta_m x)]}{\left\{\left(\beta_m^2 + H_1^2\right)\left[L + H_2/\left(\beta_m^2 + H_2^2\right)\right] + H_1\right\}} \times \left(T_i e^{-\alpha\beta_m^2 t} \times \left[\sin(\beta_m L) - \frac{H_1}{\beta_m}\cos(\beta_m L) + \frac{H_1}{\beta_m} \right] + \left\{ H_1 \int_0^t T_{\infty 1}(t) e^{\alpha\beta_m^2 t}\, dt + H_2[\beta_m \cos(\beta_m x) + H_1 \sin(\beta_m x)] \times \int_0^t T_{\infty 2}(t) e^{\alpha\beta_m^2 t}\, dt \right\} \right) \quad (9)$$

Both sink temperatures were represented to an accuracy of 0.001 ($R^2 > 0.99$) with fifth-order polynomials. Figure 8 shows the top and bottom surface temperatures for these convection boundary conditions with time-dependent sink temperatures.

It is apparent that the FE and analytical results are a close match for both surfaces and that there is little variation in temperature through this thin skin. The analytical model overpredicts the maximum day temperatures by about a degree; whereas at other times throughout the day, the differences between the two models is negligible. Those errors associated with the analytical model are caused by two approximations. The first, is the representation of the sink temperatures with a polynomial rather than using the exact temperatures as in the FE analysis. The second error is again related to the calculation of the β_m values and the related series approximation for cosine and sine terms used.

Radiation Boundary Conditions

To include the effects of radiation boundary conditions, a new approach was taken. The fourth-order effects of radiation were linearized, and a transformed heat transfer coefficient was developed.

Zerkle and Sunderland[21] have summarized work carried out on transient radiation temperature prediction via analytical analyses. They discuss the merits of using an equation given by Chapman[22] to obtain an approximate solution if the heat flux at the slab surface is nearly linear. In the case of radiation it is suggested that, when the

ratio of the temperature at a given position in the solid to the sink temperature is greater than approximately 0.75, the treatment of radiation as a linear flux is valid. In the current problem, the maximum temperature difference occurs at the initial temperature, $T_i = 288$ K, and at maximum sink temperature, $T_\infty = 350$ K, which implies that, because the temperature will always increase from this state due to the incoming solar flux, the minimum ratio $T_i/T_\infty = 0.82$. The assumption of linear radiation means that the radiation equation (3) would become identical to the convection equation (2), but with the heat transfer coefficient defined according to the radiation conditions, such that Eq. (2) would become

$$q = h_R(T - T_\infty) \tag{10}$$

where h_R is the radiation heat transfer coefficient.

The validity of this approximation has also been discussed by Jakob.[23] It was concluded that under the conditions as specified earlier, it could be an accurate representation of the radiation conditions. Therefore, it was determined that linear conditions could be assumed in the current case, to use the earlier developed analytical model.

First, the equation for a radiation-only boundary condition given in Eq. (3) was modified to suit the form

$$q = \sigma\varepsilon T_\infty\left[1 - (T/T_\infty)^4\right] = \sigma\varepsilon T_\infty\left[1 - (1 - T/T_\infty - 1)^4\right] \tag{11}$$

When $X = 1 - T/T_\infty$, Eq. (11) can be rewritten as

$$q = \sigma\varepsilon T_\infty^4[1 - (X - 1)^4] \tag{12}$$

The full expansion of the term $(X - 1)^4$ is given by

$$(X^4 - 4X^3 + 6X^2 - 4X + 1) \tag{13}$$

When a simple study of the influence of each term in Eq. (13) was performed, it was determined that the accuracy gained by using a quadratic representation did not justify the added complexity it would bring to the problem. In fact, it was seen that the first-order term of Eq. (13) provided over 95% of the solution, when the condition of $T_i/T_\infty > 0.75$ or, for the current case, when $X = (1 - T_i/T_\infty)$, $X < 0.25$, was met. In the current problem, the maximum value for X is 0.18; therefore, the assumption of approximately linear behavior is justified. The influence of the first term was found to grow as $X \Rightarrow 0$.

The equation for a radiation boundary condition can then be written as

$$q = \sigma\varepsilon T_\infty^4(4X) = 4\sigma\varepsilon T_\infty^4 - 4\sigma\varepsilon T_\infty^3 T \tag{14}$$

Equation (14) can be rewritten in the same form as for convection boundary conditions, such that the final form of the Fourier heat transfer equations for a radiation boundary condition, based on the aforementioned assumptions, is given by

$$-k\frac{\mathrm{d}T}{\mathrm{d}x} + h_R T = h_R T_\infty \tag{15}$$

When Eqs. (14) and (19) are compared, the radiation heat transfer coefficient h_R can be defined as

$$h_R = 4\sigma\varepsilon T_\infty^3 \tag{16}$$

Figure 9 shows the temperature distributions calculated using Eq. (9) and the new radiation heat transfer coefficient as stated in Eq. (16), through the CFRP skin subject to radiation boundary conditions at both surfaces. In Fig. 9, it can be seen that the discrepancies between the analytical and FE results at longer times are slightly larger than those of the convection analysis, this time to a maximum of approximately 6 deg at steady state. Again, this is due to the influence of the second term in Eq. (9). Because this term is more heavily affected by the heat transfer coefficients than the first term, the error associated with assuming that radiation conditions can be approximated as linear similar to convection conditions becomes more apparent.

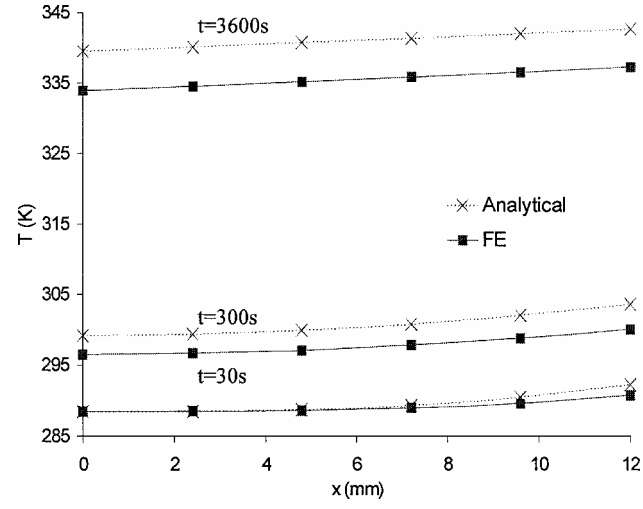

Fig. 9 Through thickness skin temperatures for radiation boundary conditions.

The use of this model with radiation boundary conditions is, however, limited to sink temperatures that are independent of time. Because the radiation heat transfer coefficient is a function of the sink temperature, every term must remain within the integral, unlike with convection-only boundary conditions. All terms containing the heat transfer coefficient must be integrated with respect to time, and due to the multiplication of these terms to the exponential function, this integration becomes extremely cumbersome. Further errors are also introduced by the approximation of the heat transfer coefficients, as well as the sink temperatures, by a polynomial. The difficulties associated with obtaining this approximation do not fit the purpose of creating simple and effective analytical models.

Combined Convection–Radiation Boundary Conditions

In reality, the conditions at a solid surface are a combination of convection and radiation. Therefore, to make the analytical model as useful as possible with respect to realistic conditions, a final case of combined convection and radiation boundary conditions at each surface is examined. For the reasons given in the radiation section, this analysis was limited to sink temperatures that were independent of time. When Eqs. (2) and (3) are combined, the general heat transfer equation for combined convection–radiation boundary conditions can first be written as

$$q = h_c(T_{\infty C} - T) + \sigma\varepsilon\left(T_{\infty R}^4 - T^4\right) \tag{17}$$

where the sink temperatures are now in terms of convection, $T_{\infty C}$, and radiation, $T_{\infty R}$, respectively. The Fourier form of Eq. (17) using Eq. (16) is

$$-k\frac{\mathrm{d}T}{\mathrm{d}x} + (h_c + h_R)T = h_c T_{\infty C} + h_R T_{\infty R} \tag{18}$$

To use the analytical model, Eq. (18) must be rewritten to fit the general form given by Eq. (4). Thus, a total combined heat transfer coefficient can be defined as

$$h = h_c + h_R \tag{19}$$

The only difficulty then, is combining the sink temperatures. Based on comparative analyses, it was determined that the most accurate representation of a combined sink temperature was the average of both the convection and radiation values. With this assumption, and by use of a combined heat transfer coefficient, Eq. (9) can then be used to perform analyses with combined convection and radiation boundary conditions. Figure 10 shows a comparison of the analytical and FE results for combined conditions.

From Fig. 10, it is evident that the model for combined boundary conditions is sufficiently accurate. The results of this combined analysis show improved agreement over that of convection-only

Table 3 Comparison of analytical and FE temperature results for convection-only, radiation-only, and combined convection–radiation boundary conditions at various analysis times[a]

	Convection			Radiation			Combined		
Surface	30 s	300 s	3600 s	30 s	300 s	3600 s	30 s	300 s	3600 s
Top	0.19	0.86	4.83	0.9	2.58	5.59	0.26	1.16	0.58
Bottom	0.26	1.32	5.36	1.44	3.52	5.38	1.39	2.52	0.88

[a]Results indicate temperature change.

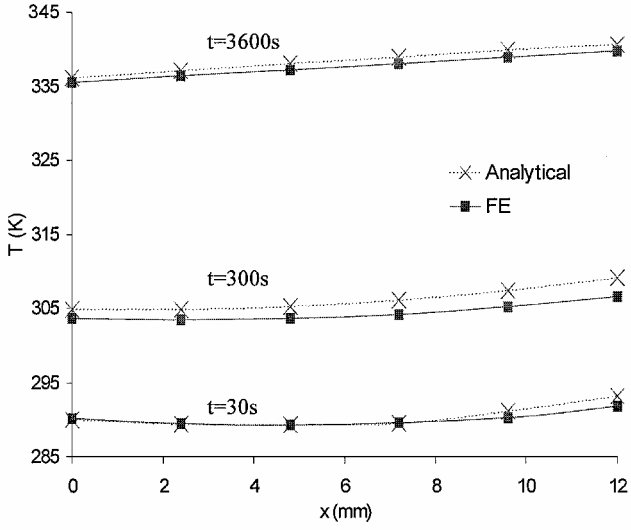

Fig. 10 Through thickness skin temperatures for combined convection–radiation boundary conditions.

and radiation-only boundary conditions. This improvement is potentially a result of the assumption of average sink temperatures. By the use of this assumption, the sink temperatures on the surfaces are lowered, in comparison to the convection-only analysis. Because the form of the analytical model is based on convection boundary conditions, this is equivalent to performing convection analysis at a slightly lower temperature; however, the FE sink temperatures were not combined and are not changed from the individual convection and radiation analyses. Thus, as the influence of the second term grows with time, the results remain closer together because of this perceived lowering of the sink temperature in the analytical analysis.

Analytical Model Conclusions

It can be concluded that the developed analytical model serves to improve confidence in the FE models, while providing an accurate, closed-form method of heat transfer analysis under certain conditions. Table 3 summarizes the maximum temperature differences between the analytical model and the respective FE model for cases of convection, radiation, and combined convection–radiation boundary conditions with sink temperatures independent of time.

From Table 3, it can be seen that the maximum difference in results occurred in the radiation-only analysis. This was expected due to the additional error incurred by assuming the radiation boundary conditions could be approximated using linear equations. The error caused by this assumption alone, however, is very small by comparison of convection-only and radiation-only results. The number of terms in the series is not a likely source of error, because, as seen in Table 2, with a reasonable number of terms, this source of error is negligible. It can be concluded, therefore, that the largest portion of error in the analytical model is caused by the sensitivity of the β_m values and the ill conditioning associated with the transcendental equation used to obtain these values. The analytical results for the convection-only and radiation-only boundary conditions were found to diverge from the FE results as time increased, to a maximum of 5 and 6 deg, respectively, at steady state. This effect was caused by the greater influence of the exponential term of Eq. (9) as time increased, which translates to a greater impact on the overall temperature predicted, due to the heat transfer coefficients and sink temperature values contained in this term. This causes the aforementioned errors associated with the analytical model to become more apparent. The analysis with combined convection–radiation boundary conditions showed a lowering of the discrepancies between the analytical and FE results, due to an assumption of an average sink temperature in the analytical model. This assumption caused the analytical analysis to be performed at a slightly lower sink temperature, thus lowering the resulting temperature profiles.

The analytical results were found to be accurate to within 5% of the FE results for all cases. It can accurately be used to model convection-only, radiation-only, and combined convection–radiation boundary conditions with the same or different heat transfer coefficients and sink temperatures at each surface. It is limited, however, in that only convection boundary conditions with time-dependent sink temperatures can be modeled efficiently. The inclusion of time-dependent heat transfer coefficients, either in convection or radiation due to a time-dependent sink temperature, cannot be modeled using the integral transform method, due to cumbersome integrations and necessary simplifying approximations.

Summary

The approach used in this paper, that of applying all three mechanisms of heat transfer within the box structure, is novel; likewise, the use of external boundary conditions in ABAQUS to include the effects of free convection within the cavity, or box, is not commonly found in commercial FE packages. The novel aspect of analytical modeling for more complex radiation and combined boundary conditions is developed. An integral transform-based technique is successfully used to model convection, radiation, and combined convection–radiation boundary conditions with different heat transfer coefficients and sink temperatures at each surface of a finite flat plate. A model for convection boundary conditions with transient sink temperatures is also developed, and the limitations and errors associated with this analytical modeling method are explored.

References

[1]Lorente, S., Petit, M., Javelas, R., "Simplified Analytical Model of Thermal Transfer in Vertical Hollow Brick," *Energy and Buildings*, Vol. 24, 1996, pp. 95–103.

[2]Globe, S., and Dropkin, D., "Natural-Convection Heat Transfer in Liquids Confined by Two Horizontal Plates and Heated from Below," *Journal of Heat Transfer*, Vol. 81, Feb. 1959, pp. 24–28.

[3]Esayed, M. M., Al-Najem, N. M., El-Rafaaee, M. M., and Noor, A. A., "Numerical Study of Natural Convection in Fully Open Tilted Cavities," *Heat Transfer Engineering*, Vol. 20, No. 3, 1999, pp. 72–85.

[4]Pessoa-Filho, J. B., and Thynell, S. T., "An Approximate Solution to Radiative Transfer in Two-Dimensional Rectangular Enclosures," *Journal of Heat Transfer*, Vol. 119, Nov. 1997, pp. 738–745.

[5]Osizik, M. N., *Boundary Value Problems of Heat Conduction*, International Textbook, Scranton, PA, 1968.

[6]Holman, J. P., *Heat Transfer*, 7th ed., McGraw–Hill, London, 1992.

[7]Eckert, E. R. G., and Drake, R. M., *Analysis of Heat and Mass Transfer*, Hemisphere, London, 1987.

[8]Schnieder, P. J., *Conduction Heat Transfer*, Addison–Wesley, Reading, MA, 1955.

[9]Carslaw, H. S., *Introduction to Mathematical Theory of the Conduction of Heat in Solids*, Macmillan, London, 1921.

[10]De Monte, F., "Transient Heat Conduction in One-Dimensional Composite Slab: A 'Natural' Analytic Approach," *International Journal of Heat and Mass Transfer*, Vol. 43, 2000, pp. 3607–3619.

[11]Antonopoulos, K. A., and Tzivanidis, C., "Analytical Solution of Boundary Value Problems of Heat Conduction in Composite Regions with Arbitrary Convection Boundary Conditions," *Acta Mechanica*, Vol. 118, 1996, pp. 65–78.

[12]Dickenson, R. D., and Martin, I. T., "Thermal Analysis of Composite Wings Using the ABAQUS Finite Element Code," BAE Systems, RN AM8623/compwing/R001, Bristol, U.K., Nov. 1999.

[13]Bolz, R. E., and Tuve, G. L., *CRC Handbook of Tables for Applied Engineering Science*, 2nd ed., CRC Press, Cleveland, OH, 1973.

[14]ABAQUS Users Manual, Ver. 5.8, Hibbitt, Karlsson, and Sorenson, Inc., Pawtucket, RI, 1999.

[15]Fujii, T., and Imura, H., "Natural-Convection Heat Transfer from a Plate with Arbitrary Inclination," *International Journal of Heat and Mass Transfer*, Vol. 15, 1972, pp. 755–767.

[16]Singh, S. N., Birkebak, R. C., and Drake, R. M., "Laminar Free Convection Heat Transfer from Downward-Facing Horizontal Surfaces of Finite Dimension," *Progress in Heat and Mass Transfer*, Vol. 2, Pergamon Press, Oxford, U.K., 1969, pp. 87–98.

[17]Vliet, G. C., "Natural Convection Local Heat Transfer on Constant-Heat-Flux Inclined Surfaces," *Journal of Heat Transfer*, Vol. 91, Nov. 1969, pp. 511–516.

[18]Catton, I., and Edwards, D. K., "Effect of Side Walls on Natural Convection Between Horizontal Plates Heated from Below," *Journal of Heat Transfer*, Vol. 89, Nov. 1967, pp. 295–299.

[19]Goldstein, R. J., and Chu, T. Y., "Thermal Convection in a Horizontal Layer of Air," *Progress in Heat and Mass Transfer*, Vol. 2, Pergamon Press, Oxford, U.K., 1969, pp. 55–74.

[20]Hollands, K. G. T., Raithby, G. D., and Konicek, L., "Correlation Equations for Free Convection Heat Transfer in Horizontal Layers of Air and Water," *International Journal of Heat and Mass Transfer*, Vol. 18, 1975, pp. 879–884.

[21]Zerkle, R. D., and Sunderland, J. E., "The Transient Temperature Distribution in a Slab Subject to Thermal Radiation," *Journal of Heat Transfer*, Vol. 87, 1965, pp. 117–132.

[22]Chapman, A. J., *Heat Transfer*, Macmillan, New York, 1960, pp. 108–121.

[23]Jakob, M., *Heat Transfer*, Vol. 1, Wiley, New York, 1949, pp. 270–291, 411–420.